

Article

Early Monitoring of Health Status of Plantation-Grown *Eucalyptus pellita* at Large Spatial Scale via Visible Spectrum Imaging of Canopy Foliage Using Unmanned Aerial Vehicles

Megat Najib Megat Mohamed Nazir ^{1,2}, Razak Terhem ^{2,3,*} , Ahmad R. Norhisham ^{2,4}, Sheriza Mohd Razali ² and Roger Meder ^{5,6} 

- ¹ Tree Plantation Division, Sabah Softwoods Berhad, Tawau 91019, Sabah, Malaysia; megatnajib91@gmail.com
² Institute Tropical Forestry and Products (INTROP), Universiti Putra Malaysia, Serdang 43400, Selangor, Malaysia; norhisham_razi@upm.edu.my (A.R.N.); sheriza@upm.edu.my (S.M.R.)
³ Laboratory of Forest Pathology and Tree Health, Faculty of Forestry and Environment, Universiti Putra Malaysia, Serdang 43400, Selangor, Malaysia
⁴ Department of Forestry Science and Biodiversity, Faculty of Forestry and Environment, Universiti Putra Malaysia, Serdang 43400, Selangor, Malaysia
⁵ Forest Industries Research Centre, University of the Sunshine Coast, Sippy Downs, QLD 4556, Australia; roger@mederconsulting.com
⁶ Meder Consulting, Bracken Ridge, QLD 4017, Australia
* Correspondence: razakterhem@upm.edu.my



Citation: Megat Mohamed Nazir, M.N.; Terhem, R.; Norhisham, A.R.; Mohd Razali, S.; Meder, R. Early Monitoring of Health Status of Plantation-Grown *Eucalyptus pellita* at Large Spatial Scale via Visible Spectrum Imaging of Canopy Foliage Using Unmanned Aerial Vehicles. *Forests* **2021**, *12*, 1393. <https://doi.org/10.3390/f12101393>

Academic Editor: Iciar Alberdi

Received: 8 July 2021

Accepted: 16 September 2021

Published: 13 October 2021

Publisher's Note: MDPI stays neutral with regard to jurisdictional claims in published maps and institutional affiliations.



Copyright: © 2021 by the authors. Licensee MDPI, Basel, Switzerland. This article is an open access article distributed under the terms and conditions of the Creative Commons Attribution (CC BY) license (<https://creativecommons.org/licenses/by/4.0/>).

Abstract: *Eucalyptus* is a diverse genus from which several species are often deployed for commercial industrial tree plantation due to their desirable wood properties for utilization in both solid wood and fiber products, as well as their growth and productivity in many environments. In this study, a method for monitoring the health status of a 22.78 ha *Eucalyptus pellita* plantation stand was developed using the red-green-blue channels captured using an unmanned aerial vehicle. The ortho-image was generated, and visual atmospheric resistance index (VARI) indices were developed. Herein, four classification levels of pest and disease were generated using the VARI-green algorithm. The range of normalized VARI-green indices was between -2.0 and 2.0 . The results identified seven dead trees (VARI-green index -2 to 0), five trees that were severely infected (VARI-green index 0 to 0.05), 967 trees that were mildly infected (VARI-green index 0.06 to 0.16), and 10,090 trees that were considered healthy (VARI-green index 0.17 to 2.00). The VARI-green indices were verified by manual ground-truthing and by comparison with normalized difference vegetation index which showed a mean correlation of 0.73 . This study has shown practical application of aerial survey of a large-scale operational area of industrial tree plantation via low-cost UAV and RGB camera, to analyze VARI-green images in the detection of pest and disease.

Keywords: *Eucalyptus*; health status; VARI-green; aerial survey; pest; disease

1. Introduction

Plantations of genus *Eucalyptus* L'Hér now amount to more than 20 million hectares globally [1] and are the second largest global forest plantation species behind *Pinus* L. [2]. Their capability for fast growth, ability to grow in a range of site conditions, ease of propagation, and their desirable wood qualities have led to widespread establishment of large *Eucalyptus* plantations in many countries of Southeast Asia which has over 2.5 million planted ha [3]. The wood of *Eucalyptus* is suitable for use in a variety of products, such as sawn timber, pulp, paper, civil construction, furniture and energy production purposes, and veneer or plywood production. In the Malaysian state of Sabah on Borneo Island, *Eucalyptus* species and hybrids have been shown to have high productivity and have a variety of end use potentials [4–7]. As countries increasingly restrict the access to natural forests for log supply, there are estimates that 50% of the world's hardwood harvest could

come from *Eucalyptus* plantations by 2030 [8]. In the Malaysian states of Sarawak and Sabah, industrial tree plantations are predominantly planted with *Eucalyptus pellita* F. Muell. or eucalypt hybrids. The prevalence of eucalypts in recent years is the result of a major outbreak of *Ceratocystis* among the previously dominant species, *Acacia mangium* Willd., resulting in a high rate of mortality [9–12]. The risk of pest and disease remains constant and it is therefore essential to monitor plantations to detect any potential incidence of disease. Any pest and disease outbreak in Eucalypt plantations has the potential to endanger the Malaysian forest industry, which aims to produce 75 million m³ of timber per annum to meet the raw material requirement of the Malaysian timber industry, which in the past 10 years has exported more than RM100 billion (USD24.4 billion) of wood products or 17% of Malaysia's total export [13].

To monitor for potential outbreak of pest and disease in *E. pellita* plantations, field surveys are important for pest and disease detection, however they are labor-intensive, time-consuming, and are not practical in areas with particularly steep terrain. Instead, precision agriculture techniques using high resolution remote sensing from unmanned aerial vehicles (UAV) with a variety of different sensors, or even conventional red-green-blue (RGB) cameras, would lead to cheaper and more practical monitoring of forest health [14–17]. Furthermore, rapid development of hardware and software, and improvement in the miniaturization of the sensors have led to the widespread use of UAV for obtaining higher temporal and spatial resolution [18–20]. It is now possible for UAVs to fly in excess of 20 h [21] and to cover more than 200 ha per flight [18]. This is sufficient to address the needs of most forest plantation operations which require collecting data in a shorter time, with fewer personnel and with minimal impact on the field. The use of UAV together with big data analytics and artificial intelligence provides new approaches for plant phenotyping [20,22–25] determination of plant height (growth) [26,27] to evaluate plant varieties [28] and detection of pest [29] and disease [30,31].

Several vegetation indices (VI) have been developed for remotely sensed images. They mostly cover the visible region of the spectrum (red, green, blue, the so-called RGB channels) or shortwave near-infrared (SWNIR), although the SWNIR region is ill-defined, but is commonly accepted to range from approximately 800 nm (red-edge) to 2500 nm. Given the high cost of true NIR spectral cameras that are capable of operating above ~1300 nm, most vegetation indices are actually confined to the visible and red-edge (up to around 1200 nm). One important consideration for remote sensing with UAVs is the payload weight, and this, combined with cost, further reduces the potential camera systems to simple RGB cameras. For RGB images, the visual atmospheric resistance index (VARI) green index [32] can benefit from normalized difference vegetation index (NDVI) using the ERTS-1 satellite (later Landsat-1) multispectral scanner [33,34].

Remotely sensed data have been used for plant phenotyping, including indices to assess plant health status [16–18,30,35–38]. The authors of [30] claimed that the use of UAV RGB imagery is more effective for estimation of disease resistance of potato light blight compared to visual assessments. Most recently, VARI-green provided reliable information to monitor tree health in *Eucalyptus pellita* in Indonesia [39]. Despite the potential advantages of UAV to collect high-resolution imagery, its application to detect biotic damage in forest plantation are currently rare in the literature. In this study, pest and disease symptoms in a stand of *E. pellita* were demonstrated using a similarly low-cost consumer UAV equipped with a similarly low-cost consumer RGB camera. This was an intentional decision to explore the capability of a readily available and affordable system without the need for expensive or sophisticated equipment such as hyperspectral/multispectral cameras. The aim of the study were to (1) investigate the health status of 1–2-year-old *Eucalyptus pellita* in a commercial plantation using VARI-green, (2) ground-truth the VARI-green result with proximally sensed NDVI data visual inspection, and (3) develop a range of indices of VARI-green as benchmark for detection and monitoring of health status.

2. Methods

2.1. Study Area and Tree Health Data

This study was undertaken in the industrial tree plantation of Brumas estate at Sabah Softwoods Berhad (Tawau, Sabah, located at latitude $4^{\circ}35'36''$ N and longitude $117^{\circ}45'31''$ E between 200 and 600 m elevation above sea level in the southern region of the Malaysian state of Sabah on the island of Borneo (Figure 1). The total planted area at SSB is approximately 18,000 hectares, which is predominantly *E. pellita* (60%) and *Falcataria moluccana* Barneby & Grimes (formerly *Albizia falcataria* L. Fosberg) as a secondary species (25%), along with *Eucalyptus* hybrids (5%) and conservation plantings (10%). The soil is dominated by Tanjung Lipat soil type with clay texture between 25% to 35% and Kumansi type with >40% clay content [40]. Block 42H, a commercial planting of *E. pellita* and selected for this study, was planted in May 2018, with an area of 22.78 ha at a spacing of 3 m \times 3 m (1111 stems per hectare, sph). A younger commercial planting (six-month-old *E. pellita*) was also assessed in Block 42G. In this block, a total of 4399 trees were planted in an area of 7.56 ha.



Figure 1. Location of the Sabah Softwoods Berhad, Brumas Estate, and location of Sabah within Borneo.

2.2. Early Inventory Measurement

The early inventory measurement (EIM) was completed five months after planting, while the ground-truth verification was completed after completion of the flight used for the VARI-green analysis.

In the EIM, visual inspection of *E. pellita* health was conducted at all study sites to establish ground reference dataset. Tree health inspection was undertaken by an experienced assessor who was trained and actively engaged in pest and disease survey in Sabah Softwood plantations.

The block 42H was chosen because of the young age when assessed using an unmanned aerial vehicle in November 2019 (1 year 7 months [19 months]), and the early inventory measurement (EIM) on the block which showed a variety of tree health status from virulent to dead.

2.3. Unmanned Aerial Vehicle Image Acquisition

High-resolution aerial images were acquired using an unmanned aerial vehicle (UAV) namely a Phantom 4 Pro, (Shenzhen DJI Sciences and Technologies (DJI), Shenzhen, China, Figure 2) equipped with a readily available consumer market RGB camera (Go-Pro 5, San Mateo, CA, USA) with a payload weight of 500 g. This configuration of UAV was used to obtain high spatial resolution imagery in the visible spectrum. The aerial survey

work was undertaken on 27 November 2019, with an altitude above canopy of 129 m and overlapping image swathes of 60% (forward) and 30% (side). Map Pilot for DJI software (Drones Made Easy, San Diego, CA, USA) was used to set the parameters (Table 1) for flightpath planning and control the movement and speed of the UAV. The constant ground sample distance (GSD) mode was set during the flight. A total of 178 images were obtained. The ground truth (GT) covered 24 plots (radius of 11.5 m) randomly scattered in the block which represents 4.22% of the total area (22.87 ha).



Figure 2. (a). Phantom 4 Pro UAV. (b) Researcher controlling the UAV. (c) Flight path.

Table 1. Flying path for control movement.

Pre-Processing Parameter	Values
Flying Height	129 m
Ground Sample distance	3.5 cm
Flight Line	Parallel
Camera snapping	Auto
Image Ratio	3:02
ISO	100
F-stop	4.5
Shutter	1/200 s
Capture Rates	3.02
Speed	Auto
Flight Duration	30 min

Ground truth assessments were conducted to classify infestation levels on *E. pellita* caused by pests and diseases. Tree health status was based on the following conditions: healthy (no sign of infestation on foliage and stem), moderate (distortion in foliage and shoots dieback), severe (splitting of stem with distortion and/or discoloration in foliage), and dead (trees no longer functional with discoloration of vascular tissues and wilting of foliage). These severity levels were used to demonstrate the potential of RGB remote images to distinguish health status of individual trees.

2.4. Image Processing

Images were processed using Agisoft Metashape software (Agisoft, St Petersburg, Russia) to generate ortho-images using parameters shown in Table 2, which is similar to the parameters used by Del-Campo-Sanchez et al. [18]. Three key steps were used to process the UAV images: initial processing, point cloud densification, and ortho-image generation. For initial processing, an automatic aerial triangulation (AAT) algorithm was used to refine the exterior orientation for all images ($N = 178$) in order to compute direct georeferencing for each image. Then, bundle block adjustment (BBA) was automatically performed to utilize the measured distance between points in order to generate an adjusted

relative three-dimensional (3D) coordinate system. For point cloud densification (Figure 3), the X, Y, Z position and the color information were computed based on the automatic tie points (ATP) in the initial processing stage. In ortho-image generation, digital surface models (DSM) with resolution 0.135 m were generated and used as reference for ortho-mosaic image creation. Agisoft software was used to import a third-party surface model for ortho-image generation, light detection and ranging (LIDAR), or interferometry synthetic aperture radar (IFSAR).

Table 2. Agisoft processing parameters.

Processing Parameters	Values
Alignment	
Accuracy	High
Generic Preselection	Yes
Reference Preselection	No
key point limit	40,000
Tie point limit	4000
Adaptive camera model fitting	Yes
Matching time	11 min 52 s
Alignment time	3 min 11 s
Optimization	
Parameters	F, b1, b2, cx, cy, k1-k4, p1, p2
Adaptive camera model fitting	No
Optimization time	8 s
Dense point cloud	
Points	16,653,614
Point colors	3 band (RGB), unit 8
Red	625–700 nm
Green	500–565 nm
Blue	450–485 nm
Reconstructions	
Quality	High
Depth filtering	Mild
Depth maps generation time	2 h 34 min
Dense cloud generation time	3 h 51 min
Total Raw Images	178 Pcs

The geomatic information obtained by GSD photogrammetric techniques is in this study a minimum of 3.5 cm pixel⁻¹. The tie points for the cloud characteristics are summarized in Table 3. The setting during the flight plan met the geomatic proposed desirable quality of final ortho-mosaic product. The ortho-images covered 27.22 hectares and provided information at a resolution of 3.5 cm GSD. The volume of data obtained from this setting were summarized in Table 4.

Table 3. Detected tie point and generated dense point cloud.

Tie Point Cloud	
Point	102,671 of 108,813
Root Mean Square reprojection error	0.162116 (1.16695 pix)
Max reprojection error	0.487534 (44.9617 pix)
Mean key point size	5.71308 pix
Effective overlap	3.46308
Dense Point Cloud	
Point	21,985,408

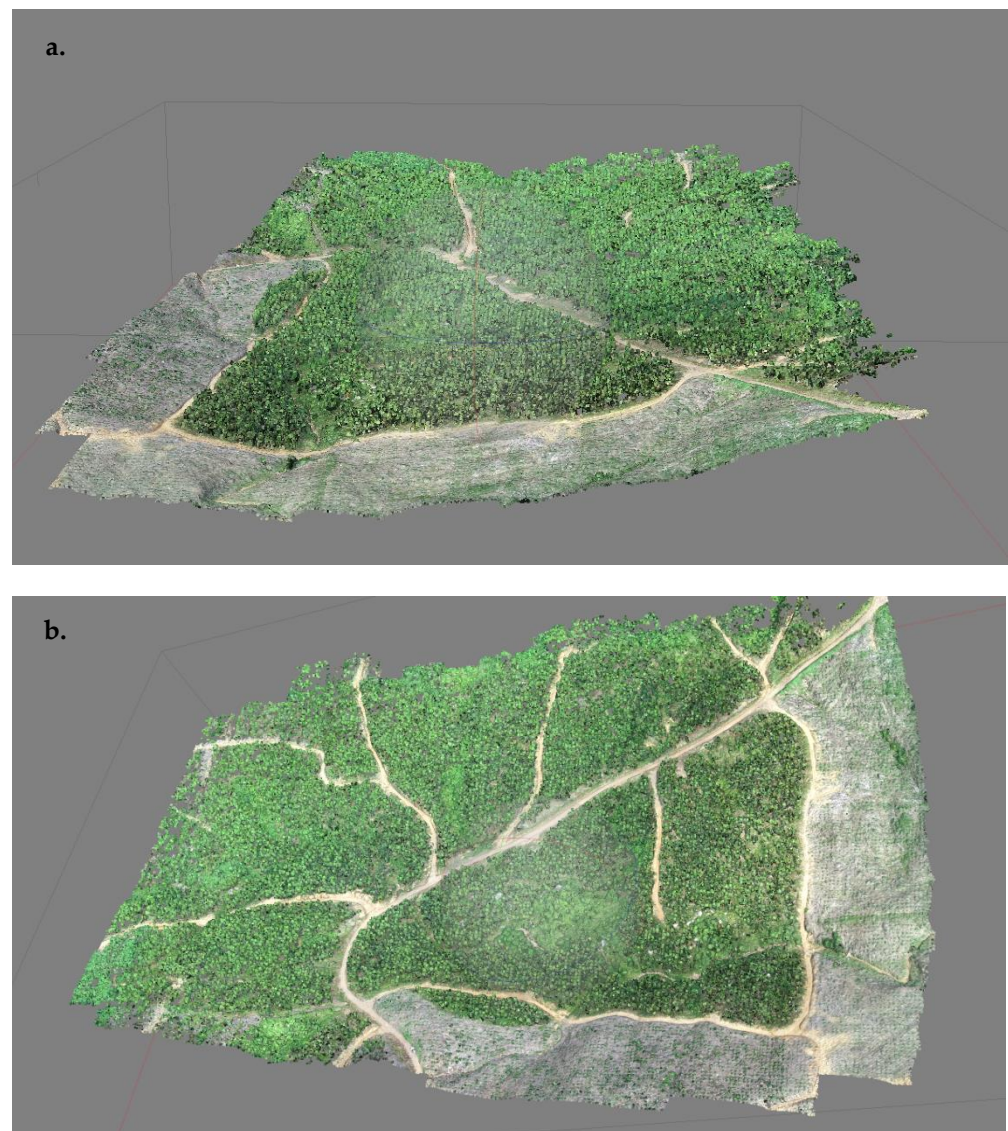


Figure 3. Point cloud densification of Block 42H. (a) Oblique view. (b) Vertical view.

Table 4. Volume of the biggest generated Geomatic products.

Geomatic Product	Size
Collected Image	178 files (1.43 gb)
Agisoft PhotoScan Project	6.11 gb
Full Orthoimage	606 mb
Nonground Orthoimage	393.40 mb
Full Orthoimage Affection Binary	-
Validation Mask	-
Red band	639.21 mb
Green band	639.21 mb
Blue band	639.21 mb

2.5. Image Analysis

Image analysis was performed using ArcGIS version 10.1 (Esri, Redlands, CA, USA). The UAV images were converted into vector shapefiles (.shp), after which, point location of the trees was plotted and buffered at a 1.0 m radius using the editor and multiple ring buffer tools. Forest blocks, roads, and stream features in the study area were digitized to represent the complete land cover map of Block 42H. The digitized tree was buffered to

1.0 m radius as an estimation of the *Eucalyptus* trees crown diameter affected by disease or mortality. The estimation is based on the maximum healthy tree crown diameter in Block 42H. The buffering layer were then overlaid and clipped on the VARI-green image using Extract tools. The VARI-green index is a vegetation index produced entirely in the visible region of the spectrum using the three visible channels of red (R, 564–580 nm), green (G, 534–545 nm), and blue (B, 420–440 nm) using the algorithm of [32] $((G - R)/(G + R - B))$. The index generates a greenness level, from which tree health can be determined. The higher the index level, the healthy the trees.

The processed image bands were separated into single bands of R, G, and B using “make a raster layer” in management tools. Then, the single band inserted in raster calculator using syntax dialog. The VARI-green index was computed using Spatial Analyst of Raster calculator tool then, the value was normalized with an absolute value 10 (ABX) and log was set to Log_{10} . After the soil threshold was determined, the VARI-green image was clipped using Data Analysis tools to isolate the individual trees from soil feature. Total digital value in the VARI-green image was normalized using ABX and LOG formula. Log 10 was used to raise the digital number. The range between -2 and 2 represents the damage severity levels for infected trees (light green) to healthy trees (deep green).

2.6. Zonal Statistics

Once separation between trees and soil on the VARI-green raster image is completed, the calculations of digital number were made to identify the healthy and unhealthy trees. The Zonal Statistic tools in ArcGIS 10.1 were used to calculate the digital number on the VARI-green image. With zonal statistic tools, all digital numbers on the VARI-green were calculated based on each zone dataset. A single output value is computed for every zone in the input dataset. The statistic input was recorded using Excel files for every tree on the VARI-green raster image. The digital values from the VARI-green raster ranged from -101 to 96 .

2.7. Normalized Difference Vegetation Index (NDVI)

A GreenSeeker handheld crop sensor (Trimble Inc., Sunnyvale, CA, USA) was used to measure the Normalized Difference Vegetation Index (NDVI) for each tree located in the three selected plots 1, 17, and 24. These plots were chosen because of the highest number of dead trees were recorded during the EIM.

2.8. Confusion Matrix and Kappa Coefficient

In this study, classification of tree health class was developed based on unsupervised classification available in ArcGIS software. After that, confusion matrix and kappa coefficient were derived for classification. Kappa used to calculate proposed classification method performance, which higher kappa value approaching $+1.0$ showed strong correlation between classification and validation or reference class data. Furthermore, note that Kappa is not a measure of accuracy but of agreement beyond chance, and thus chance correction is not needed [41].

The confusion matrix was created based on the individual class accuracy that was calculated by dividing the element for each class (row and column). Next, the Producers Accuracy can be generated by dividing each of the major diagonal class with total number of elements on the column of category. The User Accuracy was computed by dividing each of the major diagonal with total number of rows of the element that was classified. Then, the value of kappa coefficient can be generated by using equations below, were the nearest the kappa value to 1, represent the perfect agreement [42].

3. Results

3.1. Tree Health Data and VARI-Green Indices

In Block 42H (aged 1 year 7 months [19 months] old), a total of 11,069 *E. pellita* trees were recorded and assigned to one of the four classifications of tree health Table 5 based

on infestation levels. Seven trees were classified as dead (VARI-green index -2 to 0), five trees were severely infected (VARI-green index 0 to 0.05), 967 trees were mildly infected (VARI-green index 0.06 to 0.16), and 10,090 trees were considered healthy (VARI-green index 0.17 to 2.00). The individual overall tree health status shown in the map of Block 42H in (Figure 4).

The VARI-green analysis undertaken in the 6-month-old stand (Block 42G) was, however, unsuccessful due to the size of the tree crowns being too small for detection.

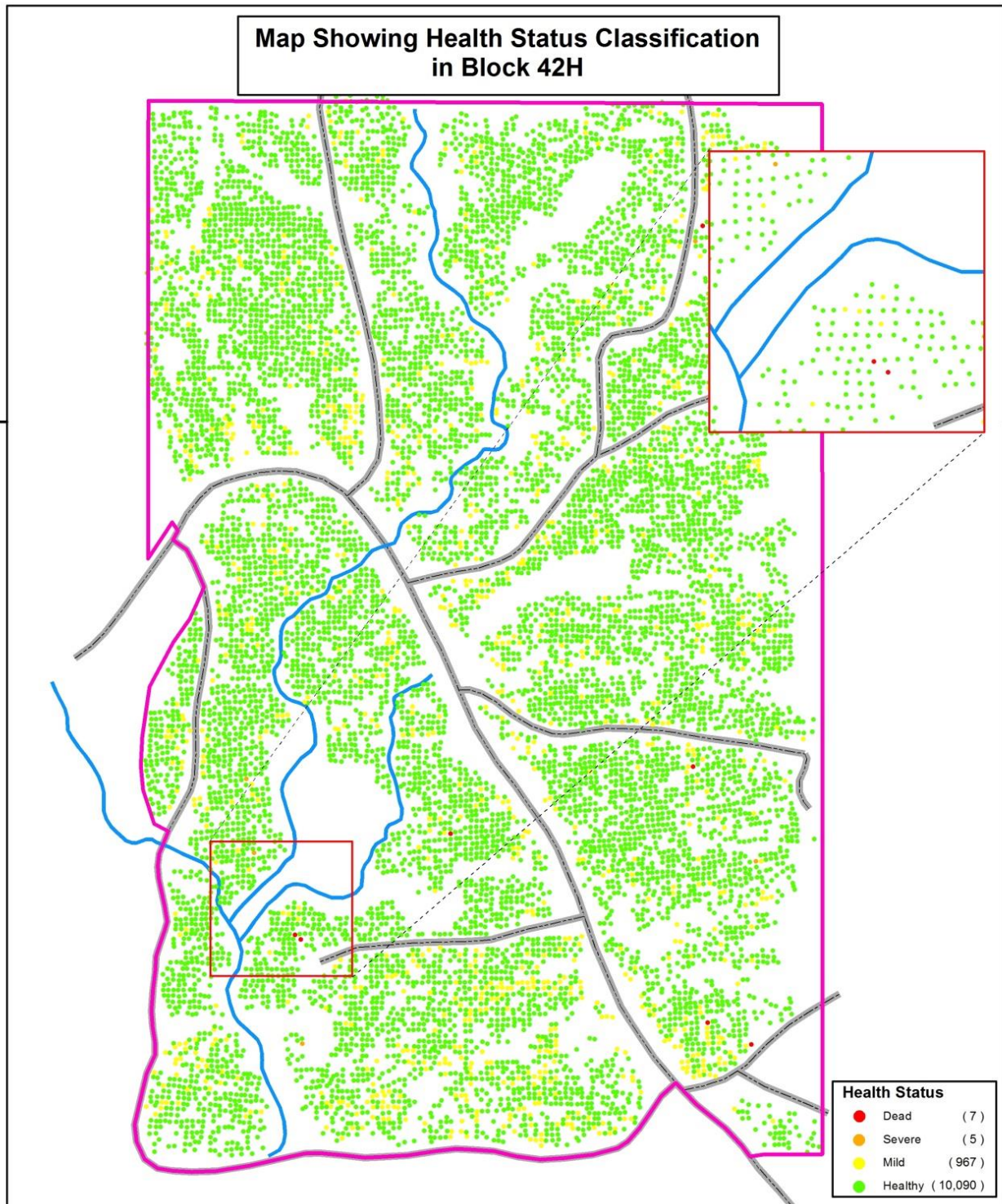
Results of 24 plots assessed in Block 42H during early inventory monitoring, ground-truthing, and after VARI-green analysis are given in Figure 5. In total, 1065 trees were recorded as living during the EIM, and 754 trees were recorded as living after VARI-green analysis. In total, 25 trees were recorded dead during the EIM and one was recorded dead after VARI-green analysis. In total, 23 trees were recorded as missing during the EIM, while 255 trees were recorded missing after VARI-green analysis. The summary ground-truth results Table 6, verified one tree as dead (Class 1) and one tree as severely infected (Class 2), respectively, while 58 trees were recorded as being mildly infected (Class 3) and 686 trees were recorded as healthy (Class 4).

The NDVI data (Supplementary Tables S1–S3) were collected to further validate the VARI-green indices data. The resulting correlation between NDVI and VARI-green showed slight differences by plot with a mean correlation value for the three trial plots of ~ 0.73 . The highest correlation value was observed in Plot 17 followed by Plot 24 and Plot 1 with values of 0.78 , 0.72 , and 0.69 respectively.

To assess the accuracy classification of tree health, we adopted a confusion matrix of the classification and kappa coefficient. The confusion matrix in Table 7 shows model prediction for each class are approximately between 60% to 100%, however class II of severe class showed very low accuracy with 0.02%. For this matrix, producer's accuracy was between 71% and 100%, meanwhile user's accuracies were between 0.0% and 98%. The overall accuracy of 0.91 succeeded in identifying almost all tree health categories with more than 90% accuracy.

Table 5. Classification of health status base on the percentage of indices value of VARI-green.

Class	Health Status	VARI-Green Value	Number of Trees	Symptoms	Causal Agent
1	Dead	$-2-0$	7	Trees no longer functional due to vascular and leaves discoloration	Pathogenic microorganism (<i>Ralstonia solanacearum</i>)
2	Severe infection	$0-0.05$	5	Splitting of trunk at stem with stippling leaves and discoloration	Stem borer (<i>Zeuzera coffeae</i> , <i>Endoclita</i> sp.) and phytophagous insects (<i>Helopeltis</i> sp.)
3	Mild infection	$0.06-0.16$	967	Distortion of foliage and shoots dieback	Sap-sucking insect (<i>Helopeltis</i> sp.)
4	Healthy	$0.17-2.00$	10,090	No sign of infestation on leaves and trunk	





SABAH SOFTWOODS BERHAD
(Formerly known as Sabah Softwoods Sdn.Bhd.)
No. Syarikat 016887-D
KM 8, Jln Sin San, pasir Putih
P.O. Box 60966, 91019 Tawau
Tel:+6 089-771333, fax:+6 089-754225,774888

Legend

- Block Boundary
- Stream
- Road

Block No.	Sur.Ha	Ptd.Ha
T. Palm	SPH	T. Road (m)
		RPH (Ch/Ha)

DRONE	: UAV
RESOLUTION	: 15 CM
ACQUISITION DATE	: 19.05.2016 - 27.06.2016
PROJECTION	: BORNEO RSO (METER)
DATUM	: TIMBALAI 1948



File Name: Ssb/Master
Printed date: 24.03.2021

Checked & Certified by:



HOD/Manager
GIS Section,
Planning, Survey & Mapping Department.

Figure 4. VARI-green result for Block 42H showing individual tree health status.

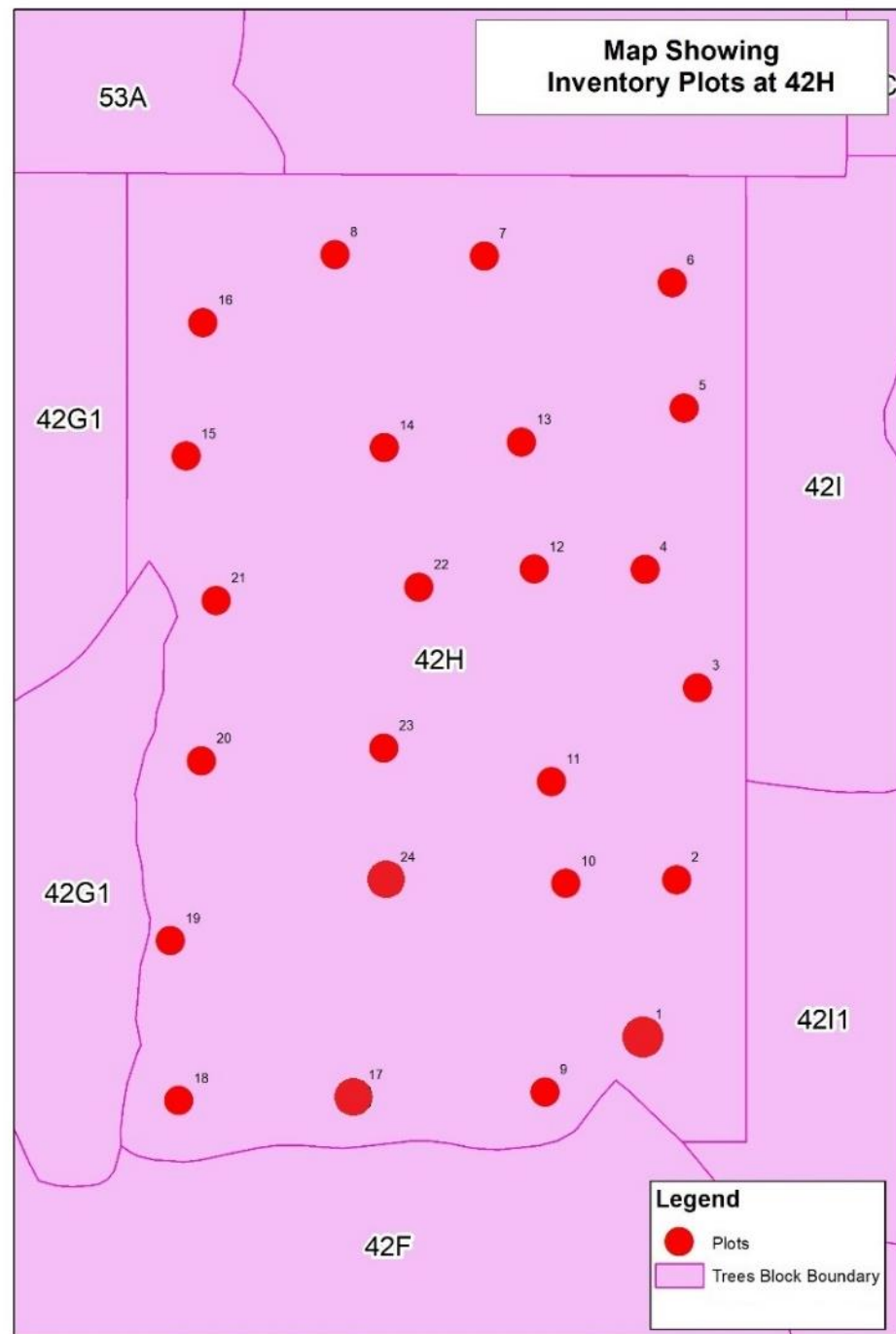


Figure 5. Schematic of the 24 inventory plots within Block 42H.

Table 6. Early monitoring measurement and results of VARI-green analysis.

Plot No.	Early Monitoring Measurement (EIM)						VARI-Green Analysis					
	Up Slope (°)	Down Slope (°)	Plot Radius (M)	Live Trees	Dead Trees	Missing Tree (Qty)	Live Trees	Dead (Class 1)	Severe (Class 2)	Mild (Class 3)	Health (Class 4)	Missing Trees (Qty)
1	5	6	11.29	37	4	4	36	1	-	8	27	10
2	23	22	11.41	41	-	2	33	-	1	1	31	9
3	33	21	11.48	41	3	1	30	-	-	-	30	15
4	38	38	11.68	46	1	1	34	-	-	-	34	11
5	22	25	11.44	46	1	-	13	-	-	-	13	14
6	5	15	11.31	46	-	-	23	-	-	3	20	16
7	28	22	11.44	47	1	2	37	-	-	-	37	8
8	15	22	11.38	43	-	-	31	-	-	1	30	12
9	21	25	11.44	49	1	-	29	-	-	-	29	11
10	40	28	11.57	46	2	1	34	-	-	4	34	11
11	25	25	11.48	46	1	-	36	-	-	-	36	7
12	25	20	11.44	48	-	-	35	-	-	5	30	6
13	30	33	11.57	48	-	-	24	-	-	1	23	14
14	26	24	11.48	47	-	1	32	-	-	-	32	9
15	25	21	11.44	46	1	2	35	-	-	1	34	11
16	38	30	11.62	45	2	-	31	-	-	4	27	12
17	27	25	11.48	35	3	4	34	-	-	13	21	5
18	30	20	11.48	43	1	1	26	-	-	-	26	14
19	23	35	11.53	51	-	-	36	-	-	2	34	10
20	30	30	11.57	48	-	-	35	-	-	-	35	6
21	17	15	11.35	43	-	-	36	-	-	3	33	6
22	12	17	11.33	45	-	-	26	-	-	6	20	11
23	17	13	11.35	39	1	2	28	-	-	5	23	12
24	17	13	11.35	39	3	2	28	-	-	1	27	15
				1065	25	23	742	1	1	58	686	255

Table 7. Confusion matrix of tree health status based on unsupervised classification for the study area.

Predict	Class 1	Class 2	Class 3	Class 4	Total	User Accuracy
Dead	7.00	1.00	0.00	0.00	8.00	0.86
Severe	0.00	5.00	67.00	154.00	226.00	0.02
Mild	0.00	1.00	939.00	627.00	1567.00	0.60
Health	0.00	0.00	156.00	9112.00	9268.00	0.98
Total	7.00	7.00	1162.00	9893.00	11,069.00	
Producer Accuracy	1.00	0.71	0.81	0.92		

3.2. Range of Index Map of VARI-Green as Benchmark for Detection of Health Status Using UAV

In this study, four classifications of health status were developed as a benchmark for detection of individual tree health (Figure 6). Classification was based on the percentage of red within the VARI-green result for each individual tree. The resulting VARI-green index values were assigned to one of the four health classes.

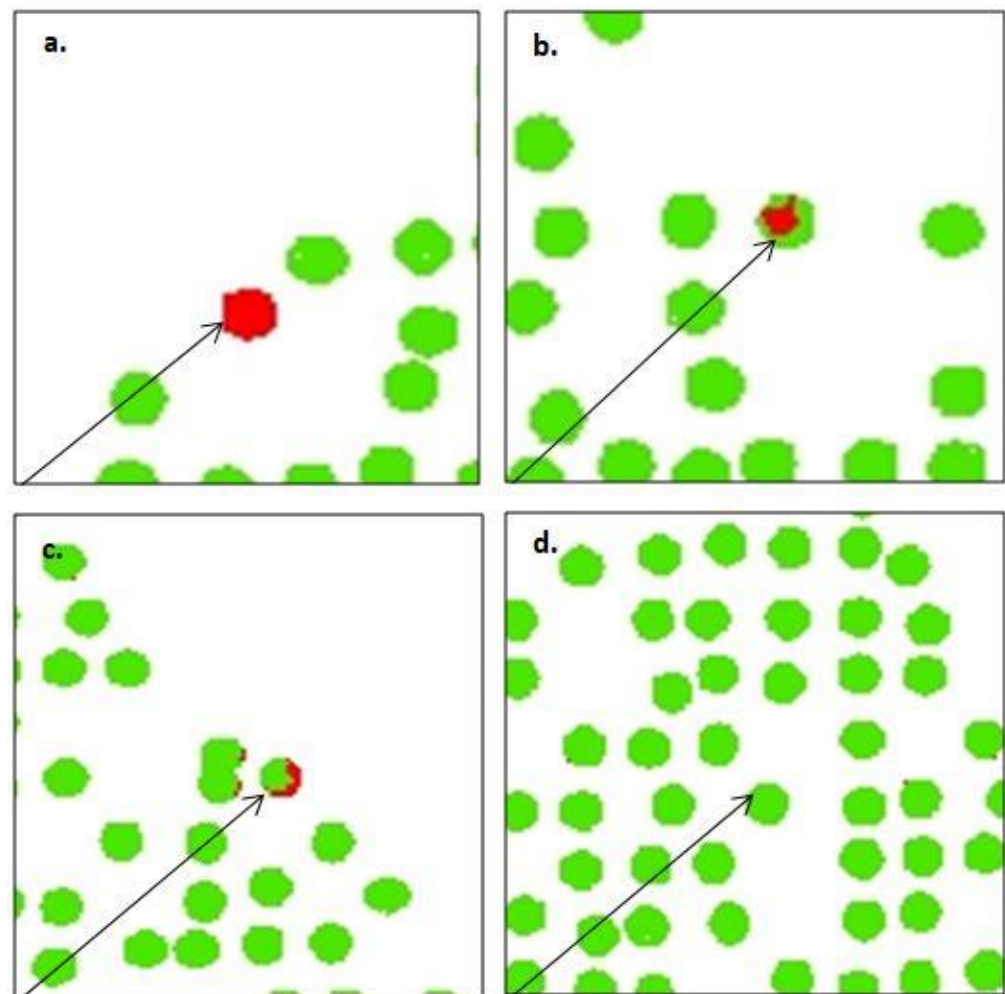


Figure 6. VARI-green classification of four health status indices: (a) Dead. (b) Severe infection. (c) Mild infection. (d) Healthy.

Figure 7 shows the procedure to generate VARI-green plots from the raw data. Orthomosaic rasters (Figure 7a) from RGB processed data clearly show the normal visualization of selected plot, from which the VARI-green raster is calculated (Section 2.5). The VARI-green raster (Figure 7b) is a result that shows the selected plot via hyperspectral visualization. To ease analysis, the tree data were isolated from soil to produce the tree-based VARI-green (Figure 7c). Due to the crowded indices data, normalized VARI-green output (Figure 7d) is produced to normalize the data between two classifications of indices, namely, 2 to 0 and 0 to -2 . From these data, the classification of tree health status was created, based on the percentage of red in the VARI-green tree crown (Figure 8).

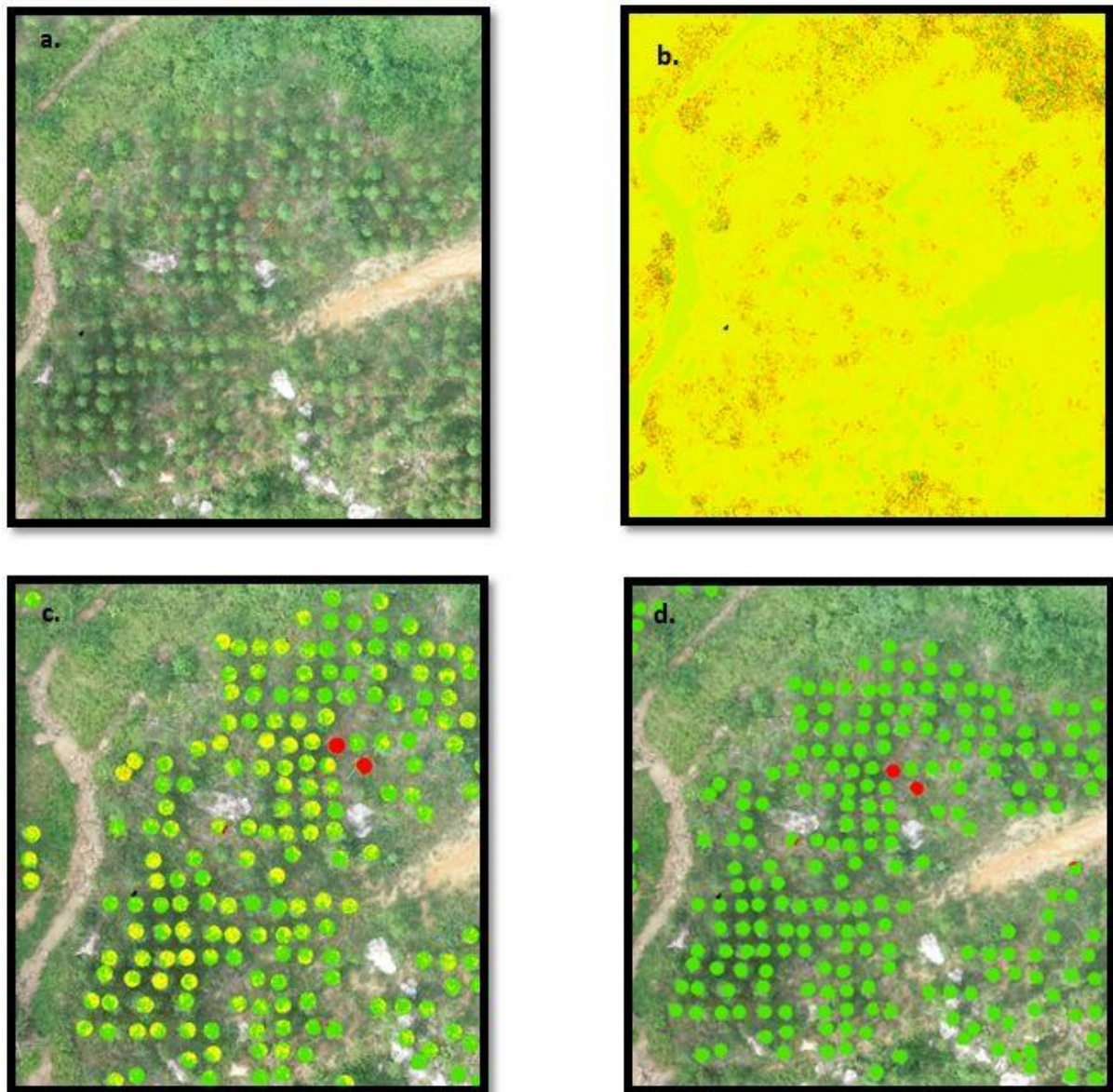


Figure 7. VARI-green image overlay with ortho-mosaic images showing the result of VARI-green from the raw data result to the normalized data result. (a) Ortho-mosaic Image Raster. (b) VARI-green raster. (c) Clipped Normalised VARI-green raster. (d) Normalised VARI-green raster.

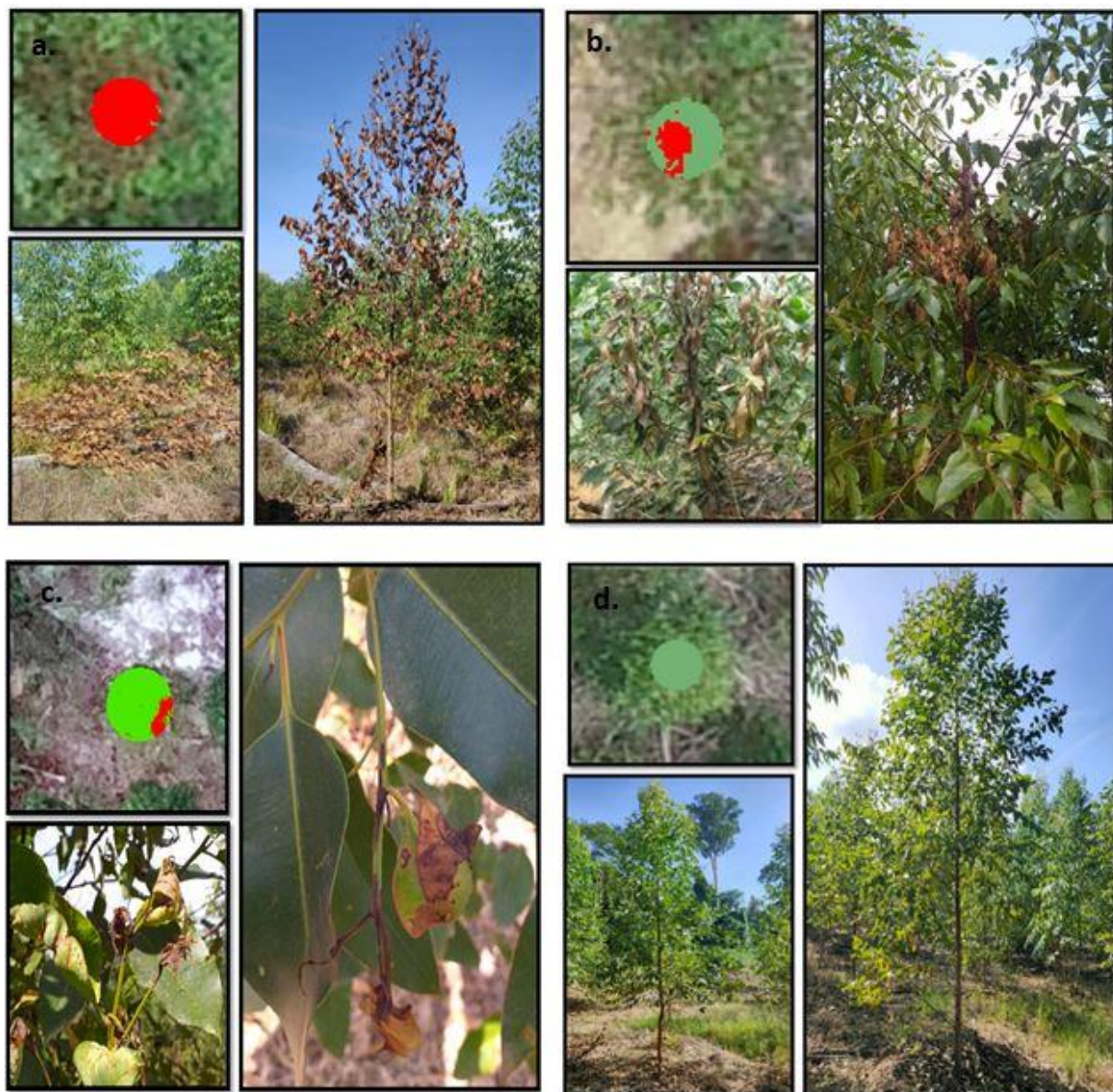


Figure 8. VARI-green and ground-truth images of (a) Class-1, dead; (b) Class-2, severe infection; (c) Class-3, mild infection; and (d) Class-4, healthy trees.

3.3. VARI-Green Pattern and Tree Health Status

The VARI-green classification map quantifies the amount of greenness in an image and differentiates between infestation levels of individual trees based on the relative amount of red in the green image. Dead trees (Class 1) appeared in the VARI-green raster pattern as totally red (Figure 8a), while severe infection (Class 2), caused in this instance by stem borer, was represented by VARI-green raster signatures with up to 80% red at the center of trees encircled by green (Class 2: Figure 8b). For mild infection (Class 3), trees show distortion in foliage and shoot dieback with VARI-green showing scattered red on individual trees (Class 3: Figure 8c). Healthy trees (Class 4) show no sign of infection on foliage and stems. The VARI-green raster pattern for Class 4 shows complete, or nearly complete, green or individual trees (Class 4: Figure 8d). Based on this variation in VARI-green pattern, the majority of trees in Block 42H are almost in perfect condition or healthy.

4. Discussion

The results of VARI (Visual Atmospheric Resistance Index) image analysis using the green channel suggest that UAV equipped with RGB cameras can be used to monitor plant health status in plantation forests. In this study, the effectiveness of a UAV equipped with a RGB camera was trialed in a young (19-month-old) stand of plantation-grown *Eucalyptus pellita* in the wet tropics in Sabah, Borneo, Malaysia. Without the need for more expensive hyperspectral cameras, simple RGB images processed using the VARI-green algorithm were able to assess pest and disease early in the growth stage. The result of this study has shown that the infestation and infection of unhealthy *E. pellita* in industrial tree plantation could be detected with the VARI-green images obtained from a low-cost drone with a low-cost RGB camera across a large area (22.78 ha). This is because VARI-green has been found to be less sensitive to atmospheric effects than NDVI, allowing a good estimation of vegetation fractions as found by [32,39].

Considering the typical host specificity of pest and disease of *E. pellita*, the classification of VARI-green images can be categorized into four classes. This classification was based on the interpretation with VARI-green index of ortho-mosaic images and ground truth verification. Confusion matrix was developed to calculate misclassification or error classification according to [43]. The result showed that our proposed methods achieve satisfactory performance, with a kappa coefficient of 0.62 and overall accuracy of 91% [44]. However, this study lacks molecular identification, while ground verification of plant health status classes is based on typical symptoms shown by the pathogen and the presence of insect pests. In the case of the dead, Class 1 *E. pellita*, the main cause of mortality was the soilborne pathogen, *Ralstonia solanacearum*. During ground inspection, dead trees exhibited leaf drop for entire the crown, branch dieback, and reduced growth. *Ralstonia* has been reported as a destructive phytopathogen that infects the xylem tissue leading to tree death [2,45] and has been reported to cause mortality in young *E. pellita* in Indonesia [39].

Based on ground verification, Class 2 was mainly caused by stem borers *Zeuzera coffeae* (Cossidae) and *Endoclita* sp. (Hepialidae) with trees showing symptoms of splitting stems and stunted growth. Attack by stem borer has been reported to interrupt nutrient transportation due to swollen stems that cause breaking of the crown top resulting in poor wood quality [46]. For Class 3, trees were infected by mirid bugs, *Helopeltis* sp. (Miridae). *Helopeltis* predominantly attack young Eucalypt leaves and shoots causing lesions, curling and drying of the foliage [47]. In addition to pest infestations, tree plantations may also suffer from water stress that causes leaf shedding however most trees retained younger leaves to cope with water deficit [48].

Overall, the early inventory monitoring results show 4% of seedling death and missing trees within the sample plots (0.96 ha) at 3 months post planting. The VARI-green data obtained 19-months post planting show 34% of seedlings as dead or missing in the sample plots (0.96 ha) from VARI-green analysis of RGB images. As a newly planted block, the trees in Block 42H are vulnerable due to their small size. They face hazards such as hot, dry weather, insect infestation, browsing by larger animals [49] or competition from vigorous weed growth although site preparation requires weed-free establishment according to Sabah Softwoods' standard operating procedure [50]. Despite this, it is accepted as normal in plantation forestry that 5–10% of the seedlings may die from one or other of these causes within the first year [49]. As shown in the results (Table 6), the high number of missing trees after VARI-green analysis compared to EIM is up to 30% may influence by several factor. The VARI-green analysis was performed 19 months post planting compared to the EIM assessment at 3 months post planting. Within this period, numerous changes have occurred in terms of tree mortality, due to any one of several biotic and/or abiotic events, e.g., drought and hot weather and infestation of pest and disease. The difference in assessment of dead and missing trees between the VARI-green result and the EIM assessment may be due to errors in either or both survey methods. The RGB images acquired by UAV may suffer from parallax error that occurs due to changes in the relative position of the object or the observation point, whereas double counting or missing counting during the manual

early inventory measurement may result in discrepancies. In this study, the VARI-green analysis and ground-truth verification in three plots were able to reduce the counting error with respect to the EIM. These results agree with those of [30] whereby the use of UAV RGB imagery is more effective for estimation of tree heath compared to visual assessments.

From a viewpoint of managing the plantation forest, VARI-green analysis indicates that only 0.06% of trees were dead and 0.04% of tree we severely infected, while 9% of the trees showed mild inhibition and 90% the trees were healthy in the total area of 22.78 ha. In terms of overall survey area, this study is amongst the largest undertaken for the detection of pest and disease in any crop: [31] covered 0.19 ha of potato crop, [39] assessed 3 ha of *E. pellita*, [30] 0.14 ha of potato crop, and [18] 5.03 ha of vineyard. The development of a health indices map combined with the practical survey of large areas shows the novelty of the study. The health indices map is easy to use, allowing plantation forest managers to view the health status of commercial forests block using comparatively low-cost technology in a rapid manner. Use of UAV to survey forest health would enable considerably larger areas to be assessed (23 ha in 30 min) compared to ground crews (10 ha per day). Aerial surveys of tree health would allow decision-making on operational procedures such as treatment of the infected area or replanting of missing trees.

Detection of early plant stress [51]; nutrient status [52]; and plant phenotyping including height, flower, and canopy cover [53] use NDVI for mapping vegetation condition and status [54]. However, NDVI requires a multispectral sensor operating in the red-edge near-infrared (NIR) wavelength range [16,17]. Near infrared cameras are more expensive than RGB cameras and require time-consuming calibration procedures [54] unlike VARI-green. VARI-green is based simply on RGB images [18] and can operate at very high resolution using low-cost UAV. This study developed plant health indices using a GoPro consumer RGB camera which was considerably cheaper than a UAV equipped with a hyperspectral camera. Though the reliability and simplicity of VARI-green has earned its popular use [54], other plant indices have been developed using conventional RGB camera. Ref. [32] found VARI-green to be minimally sensitive to atmospheric effects allowing estimation of vegetation fraction with an error of <10% in a wide range of atmospheric optical densities. This study has verified the remotely sensed VARI-green indices with proximal NDVI measures, which have shown acceptable agreement.

The total flight time of 30 min used in this study was shown to be sufficient to cover the survey area of around 23 hectares. Due to the short duration of the flight and the ease of development of plant health indices for *E. pellita*, it is proposed that UAVs with simple RGB cameras have the potential and cost effectiveness to operate in large-scale monitoring of plant health not only in Malaysia, but also within the tropical countries where *E. pellita* is grown. The study provides a methodology to assess infection on the ground with aid of remote sensing UAV image for minimal cost. It is an innovative technique that can be included in plantation management plans, not only for tree plantations, but it may also be suitable for other plantation crops such as oil palm. It is not intended that this method be a total replacement of conventional ground verification or conventional surveying methods. Instead, it is intended that aerial survey provide complementary data to rapidly and safely distinguish unhealthy areas of plantation with minimal labor cost. This would allow growers to quickly target affected areas which would be ground-truthed by trained field crews who could back-up the identification of the disease outbreak using molecular identification and morphology identification. The relationship between VARI-green and ground survey showed good agreement providing a reliable classification tool for plantation managers. The four classes of plant health status have been selected for the management to provide extra information regarding the tree's health enabling better decision-making to control pest and disease outbreaks.

While this study was proven to be reliable for *E. pellita* at a stand age of 19 months, younger trees failed to be detected by the VARI-green algorithm due to the small crown size. In a forest block of 6-month-old *E. pellita* (Block 42G), VARI-green analysis was unable to differentiate between trees, indicating that there must be a minimum canopy

size before VARI-green can produce reliable result. These findings also suggest that forest plantation deployed with species such as *Albizia* sp. and *Tectona grandis* may encounter similar problems of confounding values in VARI-green analysis due to overlapping crown.

5. Conclusions

There are competing needs for speed and ease of monitoring large areas of planted forest and the need for accuracy and precision. In a practical operation for a forest grower managing tens of thousands of hectares of planted forest, aerial survey of forest health using VARI-green from RGB imaging, is a qualitative assessment that provides information across a large area at the expense of lower accuracy. It is the relative area that is affected which is important. To determine whether 30% of an area is potentially affected does not require a high degree of accuracy: it is simply enough to know that between 25% and 35% is affected, or less than 10% or more than 50%, etc. The commercial leverage achieved by using UAV remote sensing systems to assess tree health is the ability to survey large areas in a short period of time, and even more powerfully the ability to survey remote and steep terrain safely, without the need for ground crews to be present. This study has shown that significant plantation areas (in this instance 22.78 ha.) can be surveyed in half a day.

Supplementary Materials: The following are available online at <https://www.mdpi.com/article/10.3390/f12101393/s1>, Table S1: NDVI value for each tree in Plot 1, Supplementary Table S2: NDVI value for each tree in Plot 17 and Supplementary Table S3: NDVI value for each tree in Plot 24.

Author Contributions: M.N.M.M.N., Conceptualization, Methodology, Investigation, Formal analysis, Writing, Visualization; R.T., Conceptualization, Supervision, Methodology, Writing, Funding acquisition, Review and editing; A.R.N., Supervision, Review and editing; S.M.R., Supervision, Methodology, Review and editing; R.M., Supervision, Conceptualization, Methodology, Review & editing. All authors have read and agreed to the published version of the manuscript.

Funding: This work was supported by the key program of Transdisciplinary Research Grant Scheme (TRGS 2018-1), Reference code: TRGS/1/2018/UPM/01/2/1 Ministry of Higher Education Malaysia.

Data Availability Statement: Not applicable.

Acknowledgments: Special thanks to Hardrie bin Jadil for EIM data collection and Rahim Bin Nordin as a drone pilot for this project. The study was conducted as part of the Borneo Forestry Cooperative's forest health programme, and particular support from Sabah Softwoods Bhd, for Megat Najib Megat Mohamed Nazir and for allowing access to Block 42 H and 42 G is gratefully acknowledged.

Conflicts of Interest: The authors declare no conflict of interest.

References

1. Laclau, J.P.; Mareschal, L.; Bouvet, J.M. Eucalyptus plantations. Editorial. *For. Ecol. Manag.* **2020**, *474*, 3.
2. Old, K.M.; Wingfield, M.J.; Yuan, Z.Q. A manual of Diseases of Eucalyptus in South-East Asia. *CIFOR* **2003**. [CrossRef]
3. Dell, B.; Hardy, G.; Burgess, T. Health and nutrition of plantation eucalypts in Asia. *South. For.* **2009**, 131–138. [CrossRef]
4. Hii, S.Y.; Ha, K.S.; Ngui, M.L.; Penguang, S., Jr.; Djuju, A.; Xy, T.; Meder, R. Assessment of plantation-grown *Eucalyptus pellita* in Borneo, Malaysia for solid wood utilisation. *Austr. For.* **2017**, *80*, 26–33. [CrossRef]
5. Jarapudin, Y.; Lapammu, M.; Alwi, A.; Warburton, P.; Macdonell, P.; Boden, D.; Brawner, J.T.; Brown, M.; Meder, R. Growth performance of selected taxa as candidate species for productive tree plantations in Borneo. *Austr. For.* **2020**, *83*, 29–38. [CrossRef]
6. Jarapudin, Y.; Meder, R.; Chiu, K.C.; Lapammu, M.; Alwi, A.; Ghaffariyan, M.; Brown, M. Veneering and sawing performance of plantation-grown *Eucalyptus pellita*, aged 7–23 years, in Borneo Malaysia. *Int. Wood Prod. J.* **2021**, *12*, 116–127. [CrossRef]
7. Jarapudin, Y.; Meder, R.; Lapammu, M.; Alwi, A.; Ghaffariyan, M.; Brown, M. Mechanical wood properties of plantation-grown *E. pellita* in Borneo Malaysia. Evidence of suitable properties for high-value timber end-use. *Int. Wood Prod. J.* **2021**, *72*. [CrossRef]
8. RISI. Eucalypt Sawlog Market Outlook. 2016. Available online: <https://www.risiinfo.com/product/eucalyptus-sawlog-outlook/> (accessed on 26 April 2021).
9. Roux, J.; Wingfield, M.J. Ceratocystis species: Emerging pathogens of non-native plantation Eucalyptus and Acacia species. *South. For.* **2009**, *71*, 115–120. [CrossRef]
10. Tarigan, M.; Van, W.M.; Roux, J.; Tjahjono, B.; Wingfield, M.J. Three new Ceratocystis spp. in the *Ceratocystis moniliformis* complex from wounds on *Acacia mangium* and *A. crassicarpa*. *Mycoscience* **2010**, *51*, 53–67. [CrossRef]
11. Tarigan, M.; Wingfield, M.J. A new wilt and die-back disease of *Acacia mangium* associated with *Ceratocystis manginecans* and *C. acaciivora* sp. nov. in Indonesia. *South Afr. J. Bot.* **2011**, *77*, 292–304. [CrossRef]

12. Brawner, J.T.; Japarudin, Y.; Lapammu, M.; Rauf, R.; Boden, D.I.; Wingfield, M.J. Evaluating the inheritance of *Ceratocystis acaciivora* symptom expression in a diverse *Acacia mangium* breeding population. *South. For.* **2015**, *77*, 83–90. [[CrossRef](#)]
13. MPIC. *National Timber Industry Policy, 2009–2020*; Ministry of Plantation Industry and Commodities Malaysia: Putrajaya, Malaysia, 2009; 128p.
14. Lee, W.S.; Alchanatis, V.; Yang, C.; Hirafuji, M.; Moshou, D.; Li, C. Sensing technologies for precision specialty crop production. *Comp. Electr. Agric.* **2010**, *74*, 2–33. [[CrossRef](#)]
15. Garcia-Ruiz, F.; Sankaran, S.; Maja, J.M.; Lee, W.S.; Rasmussen, J.; Ehsani, R. Comparison of two aerial imaging platforms for identification of Huanglongbing-infected citrus trees. *Comp. Electr. Agric.* **2013**, *91*, 106–115. [[CrossRef](#)]
16. Dash, J.P.; Watt, M.S.; Pearse, G.D.; Heaphy, M.; Dungey, H.S. Assessing very high resolution UAV imagery for monitoring forest health during a simulated disease outbreak. *ISPRS J. Photogram. Rem. Sens.* **2017**, *131*, 1–14. [[CrossRef](#)]
17. Abdollahnejad, A.; Panagiotidis, D. Tree species classification and health status assessment for mixed broadleaf-conifer forest with UAS multispectral imaging. *Rem. Sens.* **2020**, *12*, 3722. [[CrossRef](#)]
18. Del-Campo-Sanchez, A.; Moreno, M.; Ballesteros, R.; Hernandez-Lopez, D. Geometric characterization of vines from 3D point clouds obtained with laser scanner systems. *Rem. Sens.* **2019**, *11*, 2365. [[CrossRef](#)]
19. Stark, B. Optimal Remote Sensing with Small Unmanned Aircraft Systems and Risk Management. Ph.D. Thesis, University of California Merced United States America, 2017. Stark_ucmerced_1660D_10275. Available online: [https://escholarship:uc/item/83v8v082](https://escholarship.uc/item/83v8v082) (accessed on 18 December 2020).
20. Ballesteros, R.; Ortega, J.F.; Hernández, D.; Moreno, M.A. Applications of georeferenced high-resolution images obtained with unmanned aerial vehicles Part I: Description of image acquisition and processing. *Precis. Agric.* **2014**, *15*, 579–592. [[CrossRef](#)]
21. Sattar, F.; Tamatea, L.; Nawaz, M. Droning the pedagogy: Future prospect of teaching and learning. *Int. J. Educ. Pedag. Sci.* **2017**, *11*, 62017.
22. LeCun, Y.; Bengio, Y.; Hinton, G. Deep learning. *Nature* **2015**, *521*, 436–444. [[CrossRef](#)]
23. Kussul, N.; Lavreniuk, M.; Skakun, S.V.; Shelestov, A.Y. Deep learning classification of land cover and crop types using remote sensing data. *IEEE Geosci. Rem. Sens.* **2017**, *99*, 1–5. [[CrossRef](#)]
24. Ballesteros, R.; Ortega, J.F.; Hernández, D.; Moreno, M.A. Applications of georeferenced high-resolution images obtained with unmanned aerial vehicles Part II: Application to maize and onion crops of a semi-arid region in Spain. *Precis. Agric.* **2014**, *15*, 593–614. [[CrossRef](#)]
25. Senthilnath, J.; Kandukuri, M.; Dokania, A.; Ramesh, K.N. Application of UAV imaging platform for vegetation analysis based on spectral-spatial method. *Comp. Electr. Agric.* **2017**, *140*, 8–24. [[CrossRef](#)]
26. Malambo, L.; Popescu, S.C.; Murray, S.C.; Putman, E.; Pugh, N.A.; Horne, D.W. Multitemporal field-based plant height estimation using 3D point clouds generated from small unmanned aerial systems high-resolution imagery. *Int. J. Appl. Earth Observ. Geoinform.* **2018**, *64*, 31–42. [[CrossRef](#)]
27. Hunt, E.R.; Rondon, S.I.; Hamm, P.B.; Turner, R.W.; Bruce, A.E.; Brungardt, J.J. Insect detection and nitrogen management for irrigated potatoes using remote sensing from small unmanned aircraft systems. In Proceedings of the SPIE Commercial and Scientific Sensing and Imaging, Baltimore, MD, USA, 17–21 April 2016. 98660N. [[CrossRef](#)]
28. Ampatzidis, Y.; Partel, V.; Meyering, B.; Albrecht, U. Citrus rootstock evaluation utilizing UAV-based remote sensing and artificial intelligence. *Comp. Electr. Agric.* **2019**, *164*. [[CrossRef](#)]
29. Abdulridha, J.; Batuman, O.; Ampatzidis, Y. UAV-based remote sensing technique to detect citrus canker disease utilizing hyperspectral imaging and machine learning. *Rem. Sens.* **2019**, *11*, 1373. [[CrossRef](#)]
30. Sugiura, R.; Tsuda, S.; Tamiya, S.; Itoh, A.; Nishiwaki, K.; Murakami, N.; Shibuya, Y.; Hirafuji, M.; Nuska, S. Field phenotyping system for the assessment of potato late blight resistance using RGB imagery from an unmanned aerial vehicle. *Biosyst. Engineer.* **2016**, *148*, 1–10. [[CrossRef](#)]
31. Rodríguez, J.; Lizarozo, I.; Prieto, F.; Angulo-Morales, V. Assessment of potato late blight from UAV-based multispectral imagery. *Comp. Electr. Agric.* **2021**, *184*, 106061. [[CrossRef](#)]
32. Gitelson, A.A.; Kaufman, Y.; Stark, R.; Rundquist, D. Novel algorithms for remote estimation of vegetation fraction. *Rem. Sens. Environ.* **2002**, *80*, 76–87. [[CrossRef](#)]
33. Rouse, J.W.; Haas, R.H.; Schell, J.A.; Deering, D.W. Monitoring vegetation systems in the great plains with ERTS. *NASA Spec. Publ.* **1974**, *351*, 309.
34. Braun, M.; Herold, M. Mapping imperviousness using NDVI and linear spectral unmixing of ASTER data in the Cologne-Bonn region (Germany). In Proceedings of the SPIE 10th International Symposium on Remote Sensing, Barcelona, Spain, 8–12 September 2004; p. 5239. [[CrossRef](#)]
35. Peña, J.; Torres-Sánchez, J.; Serrano-Pérez, A.; De Castro, A.I.; López-Granados, F. Quantifying Efficacy and Limits of Unmanned Aerial Vehicle (UAV) Technology for weed seedling detection as affected by sensor resolution. *Sensors* **2015**, *15*, 5609–5626. [[CrossRef](#)] [[PubMed](#)]
36. Candiago, S.; Remondino, F.; Giglio, M.; Dubbini, M.; Gattelli, M. Evaluating multispectral images and vegetation indices for precision farming applications from UAV images. *Rem. Sens.* **2015**, *7*, 4026–4047. [[CrossRef](#)]
37. Yue, J.; Lei, T.; Li, C.; Zhu, J. The application of unmanned aerial vehicle remote sensing in quickly monitoring crop pests. *Intell. Autom. Soft Comput.* **2012**, *18*, 1043–1052. [[CrossRef](#)]

38. Rasmussen, J.; Ntakos, G.; Nielsen, J.; Svensgaard, J.; Poulsen, R.N.; Christensen, S. Are vegetation indices derived from consumer-grade cameras mounted on UAVs sufficiently reliable for assessing experimental plots? *Europ. J. Agron.* **2016**, *74*, 75–92. [[CrossRef](#)]
39. Dell, M.; Stone, C.; Osborn, J.; Glen, M.; McCoul, C.; Rimbawanto, A.; Tjahyono, B.; Mohammed, C. Detection of necrotic foliage in young *Eucalyptus pellita* plantation using unmanned aerial vehicle RGB photography—A demonstration concept. *Austr. For.* **2019**, *82*, 80–86. [[CrossRef](#)]
40. Marto, A.; Yusoff, S.M. *Major Soil Type, Soil Classification, And Soil Maps*; CRC Press: Boca Raton, FL, USA, 2017; p. 224. ISBN 978-1138-19769-5.
41. Giles, M.F. Explaining the unsuitability of the kappa coefficient in the assessment and comparison of the accuracy of thematic maps obtained by image classification. *Remote. Sens. Environ.* **2020**, *239*, 0034–4257. [[CrossRef](#)]
42. L3Hariss Geospatial Home Page. Available online: <https://www.l3harrisgeospatial.com/docs/calculatingconfusionmatrices.html> (accessed on 4 September 2021).
43. Fleiss, J.L.; Cohen, J.; Everitt, B.S. Large sample standard errors of kappa and weighted kappa. *Psychol. Bull.* **1969**, *72*, 323–327. [[CrossRef](#)]
44. McHugh, M.L. Interrater reliability: The kappa statistic. *Biochem. Med.* **2012**, *22*, 276–282. [[CrossRef](#)]
45. Carstensen, G.D.; Venter, S.N.; Wingfield, M.J.; Coutinho, T.A. Two *Ralstonia* species associated with bacterial wilt of *Eucalyptus*. *Plant Pathol.* **2017**, *66*, 393–403. [[CrossRef](#)]
46. Suheri, M.; Haneda, N.F.; Jung, Y.H.; Sukeno, S.; Moon, H.K. Effectiveness of pheromone traps for monitoring *Zeuzera* sp. (Lepidoptera: Cossidae) population on *Eucalyptus pellita* plantation. *IOP Conf. Ser. Earth Environ. Sci.* **2020**, *468*, 012016. [[CrossRef](#)]
47. Kodakkadan, S.; Yeshwanth, H.M.; de Souza Tavares, W.; Pasaribu, I.; Abad, J.I.M.; Tarigan, M.; Duran, A.; Yong, W.C.; Sharma, M. Mirid pests of *Eucalyptus* in Indonesia: Notes on damage symptoms, alternate hosts and parasitoid. *J. Kansas Entomolog. Soc.* **2020**, *92*, 577–588. [[CrossRef](#)]
48. Gindaba, J.; Rozanov, A.; Negash, L. Response of seedlings of two *Eucalyptus* and three deciduous tree species from Ethiopia to severe water stress. *For. Ecol. Manag.* **2004**, *201*, 119–129. [[CrossRef](#)]
49. West, P.W. *Growing Plantation Forests*, 2nd ed.; Springer International Publishing: Basel, Switzerland, 2014; 329p, ISBN 978-3-319-01827-0.
50. Alwi, A.; Lapammu, M.; Japarudin, Y.; Molony, K.; Boden, D.; Macdonell, P.; Warburton, P.; Brawner, J.T.; Meder, R. Importance of weed control prior to planting for the establishment of planted forests in Sabah, Malaysia. *J. Trop. For. Sci.* **2020**, *32*, 349–354. [[CrossRef](#)]
51. Beisel, N.S.; Callahan, J.B.; Sng, N.J.; Taylor, D.J.; Paul, A.L.; Ferl, R.J. Utilization of single-image normalized difference vegetation index (SI-NDVI) for early plant stress detection. *Appl. Plant Sci.* **2018**, *19*, e01186. [[CrossRef](#)] [[PubMed](#)]
52. Caturegli, L.; Corniglia, M.; Gaetani, M.; Grossi, N.; Magni, S.; Migliazzi, M.; Angelini, L.; Mazzoncini, M.; Silvestri, N.; Fontanelli, M.; et al. Unmanned aerial vehicle to estimate nitrogen status of turfgrasses. *PLoS ONE* **2016**. [[CrossRef](#)]
53. Xu, R.; Li, C.; Paterson, A.H. Multispectral imaging and unmanned aerial system for cotton plant phenotyping. *PLoS ONE* **2019**. [[CrossRef](#)]
54. Costa, L.; Nunes, L.; Ampatzidis, Y. A new visible band index (vNDVI) for estimating NDVI value on RGB images utilizing genetic algorithms. *Comp. Electr. Agric.* **2020**, *172*, 105334. [[CrossRef](#)]